P H Y S I C A L   R E V I E W   L E T T E R S

Efficient Quantum-State Estimation by Continuous Weak Measurement and Dynamical Control

Greg A. Smith,[1] Andrew Silberfarb,[2] Ivan H. Deutsch,[2] and Poul S. Jessen[1]

[1]*College of Optical Sciences, University of Arizona, Tucson, Arizona 85721, USA*
[2]*Department of Physics and Astronomy, University of New Mexico, Albuquerque, New Mexico 87131, USA*
(Received 12 June 2006; published 31 October 2006)

We demonstrate a fast, robust, and nondestructive protocol for quantum-state estimation based on continuous weak measurement in the presence of a controlled dynamical evolution. Our experiment uses optically probed atomic spins as a test bed and successfully reconstructs a range of trial states with fidelities of ~90%. The procedure holds promise as a practical diagnostic tool for the study of complex quantum dynamics, the testing of quantum hardware, and as a starting point for new types of quantum feedback control.

Fast, accurate, and robust quantum-state estimation (tomography) is important for the study of complex quantum systems and dynamics and promises to be an essential tool in the design and testing of hardware for quantum-information processing [1]. Previous demonstrations range from optical [2] to atomic [3] and molecular systems [4], but with some exceptions in the fields of quantum optics and nuclear magnetic resonance, the procedures have been too cumbersome to find much use. Quantum-state estimation is usually formulated in terms of strong measurements of an informationally complete set of observables [5]. While appealing from an information-theoretical perspective, this approach often translates poorly in a laboratory setting where it may be difficult or impossible to implement the desired measurements in practice. Furthermore, strong measurements erase the original quantum state, and the ensemble must be reprepared and the measurement apparatus reconfigured at each step. Here we demonstrate an alternative approach based on continuous weak measurement and dynamical control [6] that sidesteps these difficulties. Using a weak measurement spreads quantum backaction across the ensemble and dilutes it to the point where it does not significantly affect any individual member. In the absence of backaction, the quantum state remains largely intact, subject only to minimal damage from errors in the external drive fields and coupling to the environment. This allows us to estimate the state in a single interrogation of the ensemble, based on the measurement of a convenient single observable O and a carefully designed system evolution.

In the Heisenberg picture, the chosen dynamics leads to a time-dependent observable, $O \rightarrow O(t)$, and the measurement history can be made informationally complete if the system is *controllable*, i.e., the dynamics can generate any unitary in $SU(d)$, where d is the dimensionality of Hilbert space. With a nondestructive measurement and near-reversible dynamics, the entire ensemble remains available at the end of the estimation procedure, in a known quantum state that can be restored close to its initial form if desired. In principle, this means that the knowledge gained can be used as a basis for further action, for example, real-time

feedback control [7] or error correction [1]. From a practical viewpoint, our procedure is highly efficient: the ~1 ms interrogation time is limited only by the control and measurement bandwidths, and data analysis is performed offline. It is also robust, in the sense that imperfections in the experiment can be included in the analysis if known, or estimated along with the state if they fluctuate in real time.

The quantum system used in our laboratory implementation is the total spin-angular momentum (electron plus nuclear) of an atom in the electronic ground state, here the $F = 3$ hyperfine manifold of ^{133}Cs. A detailed theoretical description of our estimation procedure and how to model this system can be found in [6]. Our Cs ensemble is prepared by laser cooling and optical pumping and consists of a few million atoms in a cloud with radius ~0.3 mm. The spins are coupled to the polarization of an off-resonance probe beam that serves as a meter for the measurement and can be read out in an arbitrary basis with a shot-noise limited polarimeter [8], as illustrated in Fig. 1(a). The spin-probe coupling depends on the atomic tensor polarizability and can be expressed in terms of the single-atom spin **F** and the probe Stokes vector **S**,

$$V_{\mathrm{SP}} = \xi_2[-F_z^2 S_0 + (F_x^2 - F_y^2)S_1 + (F_x F_y + F_y F_x)S_2] + \xi_1 F_z S_3, \qquad (1)$$

where the coupling constants ξ_i depend on the probe frequency, the cloud optical density, and the atomic transition [9]. Terms containing S_1, S_2, and S_3 lead to rotation of the Stokes vector around the 1, 2, and 3-axis of the Poincaré sphere, by angles proportional to the ensemble-averaged values of the respective spin observables. We use a probe initially polarized along the x-axis, corresponding to an input Stokes vector $\mathbf{S}_{\mathrm{in}} = S_0(1, 0, 0)$, and measure the induced ellipticity, or S_3 component of the output. For the moderate optical density clouds used here, all angles of rotation are small, the polarization measurement is sensitive only to rotations around the 2-axis, and the measured observable is $O = F_x F_y + F_y F_x$. Coupling the entire spin ensemble to a common probe can, in principle, produce
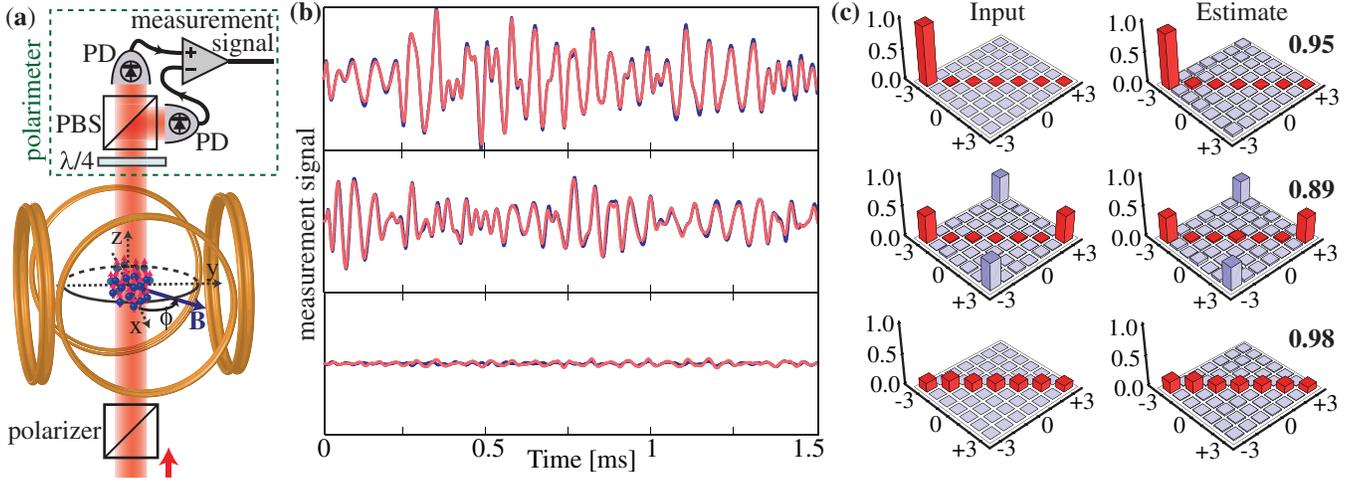
FIG. 1 (color online).   Continuous measurement and quantum-state estimation for atomic spins. (a) Schematic of our experiment. PBS: polarization beamsplitter; PD: photodetector; $\lambda/4$: quarter-wave plate. The control magnetic field has constant magnitude and is confined to the x-y plane; the time-dependent angle ϕ is optimized for best estimation fidelity. (b) Simulated (dark line) and observed (light line) measurement signals for test states $|m_F = -3\rangle$ (top), $|\psi_c\rangle$(middle) and ρ_{mix} (bottom). (c) Input and estimated density matrices (absolute values) corresponding to the simulated and observed measurement signals.

correlations between individual spins [10], but this effect is negligible for our optical densities.

To extract information, we evolve the spins to obtain a time varying observable $O(t)$. Coarse-graining over time yields a discrete set $\{O_i\}$ and a measurement record $\{M_i\}$, where $M_i = \mathrm{Tr}[O_i\rho_0] + \Delta M$. Here, ρ_0 is the quantum state to be estimated, and ΔM is a Gaussian white noise process dominated by probe shot noise. Full system controllability is required to make $\{O_i\}$ informationally complete and can be achieved with a Hamiltonian of the form $H_s(t) = g_f\mu_B\mathbf{B}(t)\cdot\mathbf{F} + \beta\hbar\gamma_s F_x^2$ produced by a time-dependent magnetic field and the probe-induced tensor light shift [Eq. (1)] [11]. Given enough time, such Hamiltonians can generate all unitaries in $SU(2F + 1)$ since the entire Lie algebra is generated by repeated commutators and linear combinations of these operators [12]. Note that for alkali atoms with an $nS_{1/2}$ electronic ground state, the tensor light shift is proportional to the photon scattering rate γ_s and therefore comes at the cost of decoherence. By probing Cs atoms on the D_1 line, we achieve $\beta = 8.2$, enough to allow significant coherent evolution before optical pumping affects the spin state. We model our system dynamics with a master equation that fully accounts for optical pumping and experimental imperfections. The latter include bandwidth limits for our magnetic coil drivers and detection system, a 6% spatial inhomogeneity in the magnitude of the light shift which can be independently estimated, and a $\sim$1% drift in our magnetic coil calibrations which must be included as free parameters in the estimation procedure.

We have evaluated the performance of our state estimation procedure by applying it to a range of test states. Nearly pure test states with $m_F = 0, \pm F$ were produced

by optical pumping and verified by Stern-Gerlach measurements of the magnetic populations. Geometric rotations of these states were obtained by Larmor precession, and more general test states were produced by evolving the system with a magnetic field and the tensor light shift. A strongly mixed state was obtained by omitting the optical pumping step and working directly with the laser cooled sample. Figure 1(b) compares the measurement record observed in a single ensemble interrogation to the one predicted by our model, for three representative inputs corresponding to a spin-polarized state $|m_F = -3\rangle$, a coherent superposition $|\psi_c\rangle = \frac{1}{\sqrt{2}}(|m_F = 3\rangle + i|m_F = -3\rangle)$, and a nearly maximally mixed state $\rho_{\mathrm{mix}} \sim I/7$. Two key features are immediately apparent: the measurement records differ substantially for different input states, and the observed and calculated measurement records agree very closely. Both conditions are clearly necessary for the procedure to generate unique and accurate state estimates.

Based on our model, we can determine the probability distribution for the measurement record, $P(\{M_i\}|\{\rho_0, p_k\})$, conditioned on the initial quantum state ρ_0 and any unknown experimental parameters p_k. We use this to obtain a maximum likelihood estimate ρ_{ML} for the state, corresponding to the peak of the posterior distribution, $P(\{\rho_0, p_k\}|\{M_i\}) = AP(\{M_i\}|\{\rho_0, p_k\})P(\{\rho_0, p_k\})$, where $P(\{\rho_0, p_k\})$ is the prior information and A is a normalization constant. Here we include as prior information only that ρ_0 must be a physical state, i.e., a positive Hermitian operator with unit trace. The conditional distribution $P(\{M_i\}|\{\rho_0, p_k\})$ is a multiparameter Gaussian centered on ρ_{LS}, the ordinary least-squares fit to the measurement record. Its covariance matrix determines the uncertainty in each of the $(2F + 1)^2$ real-valued parameters required to

specify ρ_0, and consequently how well an arbitrary state can be estimated. In setting up the procedure, the control magnetic field was optimized to minimize these widths and reduce their sensitivity to errors. In practice, the state estimate is obtained from the measurement record in a two-step process. First, we determine the least-squares fit ρ_{LS}, which is frequently nonpositive due to mismatch between the modeled and actual dynamics, and then we find the positive density matrix that lies closest to ρ_{LS}. This is our maximum likelihood estimate ρ_{ML}. Figure 1(c) compares density matrices for the input and maximum likelihood estimates for each of our three representative test states. Visual inspection clearly shows the excellent agreement achieved by our procedure. A more quantitative performance measure can be obtained by calculating the fidelity $\mathcal{F} = (\mathrm{Tr}\sqrt{\rho_0^{1/2}\rho_{ML}\rho_0^{1/2}})^2$ [13], which for these three states fall in the range 0.89–0.98. Averaging over our entire sample of test states, we achieve a mean fidelity $\bar{\mathcal{F}} \approx 0.86$ for estimates based on a single measurement record, and a slightly improved $\bar{\mathcal{F}} \approx 0.91$ for estimates based on the average of 128 measurement records. These fidelities are limited mainly by errors in the applied control fields and to a lesser degree by decoherence from probe scattering.

An alternative visualization of spin states can be given in terms of Wigner function representations [14]. Figure 2(a) shows the estimated states for six discrete time steps during Larmor precession of an initial state $|m_F = -3\rangle$. As expected for these so-called spin-coherent states, the Wigner functions resemble Gaussian "wave packets" moving on a sphere. A slight but visible sheering of the quasiprobability distribution occurs due to the F_x^2 term in the probe-induced light shift, which is expected since this is a well known mechanism for spin squeezing [15]. Figure 2(b) shows estimated states at later times when the effects of squeezing are more pronounced. As the squeezing ellipse wraps around the sphere, it eventually evolves into the coherent superposition $|\psi_c\rangle$ [16], the state used as input in Fig. 1(b) and 1(c). This series of snapshots demonstrates that our technique can be used to observe and visualize quite complex dynamical evolution.

With known input states, we can observe how the state estimate converges as the measurement record builds up. Figure 3 shows examples of the evolving fidelity and state estimate for pure and mixed inputs. In all cases, the estimation starts with an unbiased guess, corresponding to a maximally mixed state. At short times, the dynamics has explored only a small part of the set $\{O_i\}$, and the measurement record provides good information only about a few of the parameters that go into specifying the state. As a result, the estimate fluctuates randomly with each time step, subject to noise and discrepancies between model and experiment. With increasing time, the dynamics explores a larger set of observables, and the probability distributions are narrowed for every parameter. At approxi-
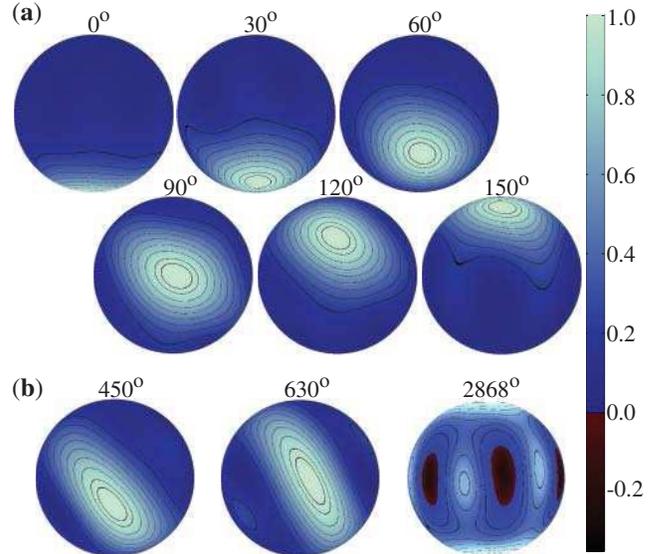

FIG. 2 (color online). Wigner function representations of an evolving spin state. (a) Snapshots of the quantum-state estimate as an initial $|m_F = -3\rangle$ state undergoes Larmor precession in the presence of the probe. The nominal precession angle θ is indicated in each case. (b) Pronounced squeezing of the spin wave packet occurs at later times, and at $\theta = 2868°$ the system has evolved into a coherent superposition $|\psi_c\rangle$ of spin-up or -down wave packets. The viewpoint is fixed, except for the snapshots at $\theta = 630°$ where it has been changed to show the wave packet on the opposite side of the sphere, and at $\theta = 2868°$ where it has been adjusted to show both lobes of $|\psi_c\rangle$.

mately 250 μs, the constraints become strong enough that only a limited family of similar density matrices are consistent with the measurement record, at which point the estimate ρ_{ML} stabilizes and the fidelity improves. Figs. 3(a) and 3(b) show the behaviors for inputs $|m_F = -3\rangle$ and $|\psi_c\rangle$, where the transition at 250 μs brings the fidelity close to its final value. The details of the jump depend on the semidefinite program solver used to enforce positivity, but it is always dramatic for pure states where the positivity requirement excludes most nearby points in parameter space. Figure 3(c) shows the behavior for an input ρ_{mix}, where most nearby points in parameter space fulfill the positivity requirement. As a result, the initial jump is less dramatic and the fidelity increases more gradually to its maximum value at the end of the measurement period.

In the Heisenberg picture, the state ρ_0 is time independent, and the estimate ρ_{ML} evolves only because more information becomes available in the measurement record. Once the measurement is complete, the estimate ρ_{ML} also becomes time independent. Because the dynamics are known, we can then transform to the Schrödinger picture, where the estimate becomes valid for any time, $\rho_0(t) \approx \rho_{ML}(t)$. During the measurement period, there is, of course, a gradual and irreversible—but entirely predictable—loss of information from the randomizing effects of optical pumping and drive field errors. As a result, an initially
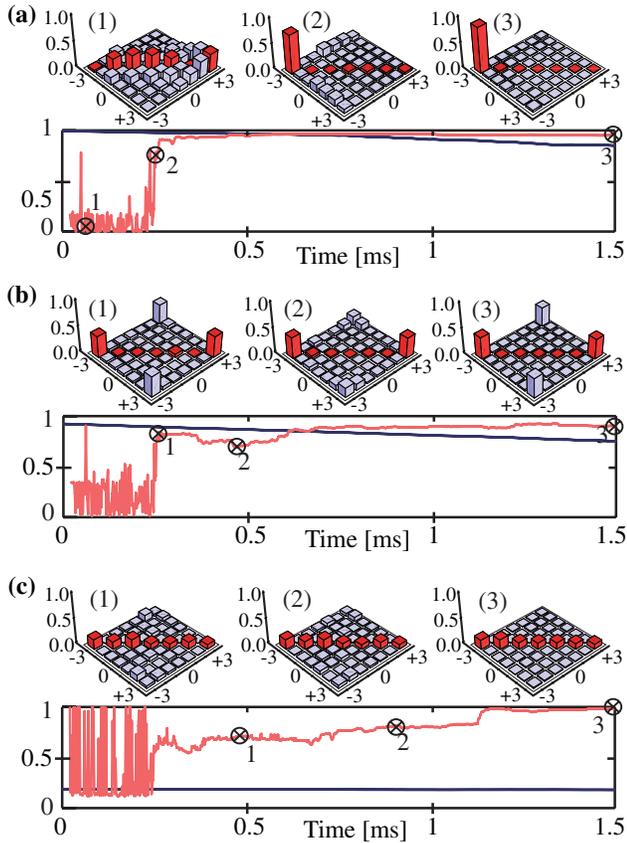
FIG. 3 (color online). Evolving fidelity, state estimate, and purity. Plots show the fidelity (light line) of the estimate ρ_{ML} and the largest eigenvalue (dark line) of the evolving state ρ_0 as a function of elapsed measurement time, for inputs (a) $|m_F = -3\rangle$, (b) $|\psi_c\rangle$ and (c) ρ_{mix}. Inserts show the estimated density matrices (absolute values only) at a few representative times.

by driving the ensemble with radio-frequency and microwave radiation in the presence of a static bias magnetic field. This would eliminate optical pumping as a source of decoherence and loss, further reduce the modest loss of state purity, and make the evolution almost completely reversible. It could also allow robust state estimation without invoking extraneous parameters and the positivity requirement for ρ_{ML}, and this could shorten our data processing time from currently $\sim 1/2$ h to perhaps a few seconds on a desktop computer. At that point, further improvements in the algorithm and computing hardware—for example the use of programmable logic devices [17]—could plausibly allow quantum-state estimation and state-based feedback control in real time.

pure state will become mixed, and the damage can be quantified by keeping track of the largest eigenvalue of $\rho_0(t)$. Figure 3 shows a small decline for the input $\sim |m_F = -3\rangle$, a slightly larger decline for the more fragile superposition $|\psi_c\rangle$, and essentially no damage to the mixed state which is already randomized. During the 1.5 ms, interrogation optical pumping transfers $\sim 10\%$ of the ensemble into the $F = 4$ manifold where atoms are invisible to the probe. This loss is included in our dynamical model and does not degrade the state estimate. Furthermore, the calculated $\rho_0(t)$ and its eigenvalues are associated only with atoms that remain in $F = 3$.

With this Letter, we have shown that fast, accurate, and nondestructive quantum-state estimation can be achieved with continuous weak measurement and dynamical control. In our current implementation, the estimation fidelity is limited by imperfect control of the slowly varying magnetic field and tensor light shift used to drive the atomic spins. Our experience suggests that it may be possible to achieve far more precise control of the atomic ground state

[1] M. A. Nielsen and I. L. Chuang, *Quantum Computation and Quantum Information* (Cambridge University Press, Cambridge, 2000).
[2] D. T. Smithey *et al.*, Phys. Rev. Lett. **70**, 1244 (1993); A. G. White *et al.*, Phys. Rev. Lett. **83**, 3103 (1999).
[3] D. Leibfried *et al.*, Phys. Rev. Lett. **77**, 4281 (1996); C. Kurtsiefer, T. Pfau, and J. Mlynek, Nature (London) **386**, 150 (1997); J. F. Kanem *et al.*, J. Opt. B **7**, S705 (2005); G. Klose, G. Smith, and P. S. Jessen, Phys. Rev. Lett. **86**, 4721 (2001).
[4] T. J. Dunn, I. A. Walmsley, and S. Mukamel, Phys. Rev. Lett. **74**, 884 (1995); E. Skovsen *et al.*, Phys. Rev. Lett. **91**, 090406 (2003); I. L. Chuang, N. Gershenfeld, and M. Kubinec, Phys. Rev. Lett. **80**, 3408 (1998).
[5] M. Paris and J. Rehacek, *Quantum State Estimation* (Springer, Berlin Heidelberg, 2004).
[6] A. Silberfarb, P. S. Jessen, and I. H. Deutsch, Phys. Rev. Lett. **95**, 030402 (2005).
[7] A. C. Doherty *et al.*, Phys. Rev. A **62**, 012105 (2000); S. Lloyd and J. E. Slotine, Phys. Rev. A **62**, 012307 (2000).
[8] G. A. Smith, S. Chaudhury, and P. S. Jessen, J. Opt. B **5**, 323 (2003).
[9] A. Silberfarb, P. S. Jessen, and I. H. Deutsch (to be published); See also J. M. Geremia, J. K. Stockton, and H. Mabuchi, Phys. Rev. A **73**, 042112 (2006).
[10] J. M. Geremia, J. K. Stockton, and H. Mabuchi, Science **304**, 270 (2004).
[11] G. A. Smith *et al.*, Phys. Rev. Lett. **93**, 163602 (2004).
[12] P. Giorda, P. Zanardi, and S. Lloyd, Phys. Rev. A **68**, 062320 (2003).
[13] A. Uhlmann, Rep. Math. Phys. **9**, 273 (1976).
[14] G. S. Agarwal, Phys. Rev. A **24**, 2889 (1981).
[15] M. Kitagawa and M. Ueda, Phys. Rev. A **47**, 5138 (1993).
[16] B. C. Sanders, Phys. Rev. A **40**, 2417 (1989).
[17] J. Stockton, M. Armen, and H. Mabuchi, J. Opt. Soc. Am. B **19**, 3019 (2002).